Metal-Organic Frameworks Post-Synthetically Modified with Ferrocenyl Groups: Framework Effects on Redox Processes and Surface Conduction

Jonathan E. Halls, Alberto Hernán-Gómez, Andrew D. Burrows*, and Frank Marken*

Department of Chemistry, University of Bath, Claverton Down, Bath BA2 7AY, UK

To be submitted to Dalton Transactions

Abstract

MOF materials based on zinc(II) and aluminium(III) dicarboxylate frameworks with covalently attached ferrocene functional redox groups were synthesised by post-synthetic modification and investigated by voltammetry in aqueous and non-aqueous media. In the voltammetry experiments, ferrocene oxidation occurs in all cases, but chemically reversible and stable ferrocene oxidation without decay of the voltammetric response requires a "mild" dichloroethane solvent environment. The voltammetric response in this case is identified as "surface-confined" with fast surface-hopping of electrons and without affecting the bulk of MOF microcrystals. In aqueous media a more complex pH-dependent multi-stage redox process is observed associated with chemically irreversible bulk oxidation and disintegration of the MOF framework. A characteristic 30 mV per pH unit dependence of redox potentials is observed attributed to a "framework effect": the hydroxide-driven MOF framework dissolution.

Keywords: MOF, post-synthetic modification, ferrocene, surface processes, pH, voltammetry, solid state electrochemistry.

1. Introduction

Metal-organic frameworks (MOFs) are a relatively new class of porous material,[1-3] and they are currently attracting considerable attention for a wide range of applications.[4] One of the enticing features of MOFs is the potential to control the shape and chemical nature of the pores, either through the use of functionalised linkers, or through use of post-synthetic modification, whereby a pre-formed MOF undergoes further reaction.[5]

The electrochemistry of MOFs is complex[6, 7] and highly interesting due to the ion insertion and expulsion processes which are expected to occur coupled to electron transfer.[8] Electrochemical studies have been carried out on systems in which either the metal centres[9, 10] or the linkers[11-13] undergo redox processes. In a recent report we investigated the redox processes associated with reduction of the commercially available iron(III) MOF Basolite F300 and discovered reductive dissolution as well as electrocatalysis at electrochemically generated surface sites.[14] Recent work by Kitagawa and co-workers has demonstrated a wider potential for MOF materials to act as designer-electrocatalysts.[15]

Ferrocene has attracted attention in MOF systems either as part of the coordination polymer backbone[16] or included as a guest within the pores.[17-21] Recently, Fischer and co-workers reported the post-synthetic modification of the bridging hydroxy group in [Al(OH)(bdc)] (MIL-53(Al)) on reaction with 1,1'-ferrocenediyl-dimethylsilane, demonstrating reversible electrochemical activity with a shift of 60 mV towards a more positive potential.[22] This material was shown to act as a redox

catalyst for benzene oxidation with aqueous hydrogen peroxide to selectively form phenol.

In this paper, we investigate MOFs based on zinc(II) and aluminium(III) which have been post-synthetically functionalised with ferrocenyl groups through an amine to amide functional group interconversion. The pores are functionalised within the MOF structure and reversible electrochemical responses are observed. The redox processes are interpreted in terms of dominating "framework effects" where aqueous media allow irreversible redox-dissolution and organic media only allow surface redox processes. Reversible ion insertion into the bulk is not observed.

2. Experimental Details

2.1. Chemical Reagents

1,2-Dichloroethane (Fisher), phosphoric acid (85 wt % in water ACS reagent), KCl, NaOH, and tetrabutylammonium hexafluorophosphate (all Sigma-Aldrich), were obtained in the highest commercially available grade and used without further purification. Compounds **1**, **2** and **4** were prepared following literature methods.[23-25] Demineralized and filtered water was taken from a Thermo Scientific water purification system (Barnstead Nanopure) with a resistivity of not less than 18 MΩ cm.

2.2. Syntheses

2.2.1 Preparation of $[Zn_4O(bpdc\text{-}NH_2)_3]$, 3.

$Zn(NO_3)_2 \cdot 6H_2O$ (0.200 g, 0.672 mmol) and 2-aminobiphenyl-4,4'-dicarboxylic acid (H_2bpdc-NH_2, 0.064 g, 0.249 mmol) were dissolved in DMF (5 cm^3), and the reaction mixture was heated at 130 °C for 24 h to give pale yellow cubic crystals. The mother liquor was removed by decantation and the crystals were washed with DMF (3 × 5 cm^3), $CHCl_3$ (5 cm^3) and soaked in $CHCl_3$ (5 cm^3) for 24 hours. Then, the crystals were rinsed with $CHCl_3$ (5 cm^3) and soaked in fresh $CHCl_3$ for 24 hours. After 3 days of washing and soaking the crystals were stored in the last $CHCl_3$ solution until needed. One sample was dried by air and weighed to give 0.0826 g (88 %). The identity of **3** was confirmed by comparison of its powder X-ray diffraction pattern to that reported by Telfer and co-workers.[26]

2.2.2 Post-synthetic modification reactions

Two methods were used, and a typical example of each is given below.

Room temperature method: The dried MOF (0.05 mmol) was placed into a vial with $CHCl_3$ (5 cm^3) and ferrocenecarboxylic anhydride (0.10 mmol). The sample was left for 3 days at room temperature, after which the reaction was quenched by removing the solvent by decantation. The sample was rinsed with $CHCl_3$ (3 × 5 cm^3) and soaked in $CHCl_3$ overnight. The rinsing and soaking was repeated for 3 days, and the sample stored under fresh $CHCl_3$. The degree of post-synthetic modification was assessed by digesting the modified MOF in DCl/d_6-DMSO and analysing the ^{1}H NMR spectra.

High temperature method: The dried MOF (0.05 mmol) was placed into a round bottomed flask with $CHCl_3$ (5 cm^3) and ferrocenecarboxylic anhydride (0.10 mmol).

The sample was heated under reflux for 3 days, after which it was cooled to room temperature, and the solvent was removed by decantation. The sample was rinsed with $CHCl_3$ (3×5 cm^3) and soaked in $CHCl_3$ overnight. The rinsing and soaking was repeated for 3 days, and the sample stored under fresh $CHCl_3$. The degree of post-synthetic modification was assessed as above.

2.3. Instrumentation

Voltammetric measurements were undertaken using a commercial potentiostat (CompactStat, Ivium Technologies B. V., The Netherlands) controlled by an AMD Athlon 64 X2 computer. A standard three-terminal electrochemical cell was used throughout, with a saturated calomel electrode (SCE) employed as a reference electrode, a 1 mm platinum wire counter electrode, and a 4.9 mm diameter basal plane pyrolytic graphite (bppg) working electrode. Prior to all voltammetric experiments, solutions were de-aerated with oxygen-free nitrogen (BOC Gases, UK). All experiments were conducted at a temperature of 20 ± 2 ^{o}C.

2.4. Preparation of the MOF-Modified Electrode

A methodology developed for microparticle voltammetry[27] was employed based on placing a 1 mg amount of sample onto a filter paper (Whatman 1) and gently rubbing the bppg electrode over the powder sample. Adhesion of the microparticle material to the graphite electrode occurred and the electrode was immersed into aqueous or organic electrolyte media for measurements.

3. Results and Discussion

3.1 Synthesis and characterisation of ferrocenyl MOFs

Post-synthetic modification has recently emerged as a powerful technique for forming functionalised MOFs,[5] and we have previously demonstrated reactions on zinc(II) MOFs.[28, 29] For this work, we sought to introduce ferrocenyl groups for electrochemical study, and used the amine to amide transformation, first reported in a MOF by Cohen and co-workers.[30] Four amine-containing MOFs were selected for conversion into ferrocenyl amides, namely $[Zn_4O(bdc\text{-}NH_2)_3$ (IRMOF-3, bdc-NH_2 = 2-amino-1,4-benzenedicarboxylate) **1**,[23] $[Zn_4O(bdc\text{-}NH_2)(btb)_{4/3}]$ (UMCM-1-NH_2, btb = 1,3,5-benzenetribenzoate) **2**,[24] $[Zn_4O(bpdc\text{-}NH_2)_3]$ (bpdc-NH_2 = 2-amino-4,4'-biphenyldicarboxylate) **3** and $[Al(OH)(bdc\text{-}NH_2)]$ (MIL-53-NH_2) **4**.[25] Compounds **1**, **2** and **4** were prepared using the previously reported methods, whereas **3** was prepared from the reaction of $Zn(NO_3)_2{\cdot}6H_2O$ with H_2bpdc-NH_2 in DMF. Telfer and co-workers have recently prepared **3** from the post-synthetic deprotection of a *tert*-butylcarbamate (NHBoc) functionalised MOF.[26] Following their approach, **3** was crystallographically characterised and shown to be non-interpenetrated. The powder X-ray diffraction pattern for our sample of **3**, prepared by direct combination of $Zn(NO_3)_2{\cdot}6H_2O$ and H_2bpdc-NH_2, is similar to that reported for the non-interpenetrated network, but given the potential for similarity in the powder X-ray patterns of interpenetrated and non-interpenetrated networks, it is difficult to judge unambiguously whether our sample of **3** is interpenetrated or not.

Post-synthetic modification reactions were undertaken using ferrocenecarboxylic anhydride, $\{CpFeC_5H_4C(O)\}_2O$, FCA (Scheme 1). For the zinc MOFs **1-3**, the

degree of modification was obtained by digesting samples of the modified materials in DCl/d_6-dmso and analysing the solutions by ^{1}H NMR spectroscopy.

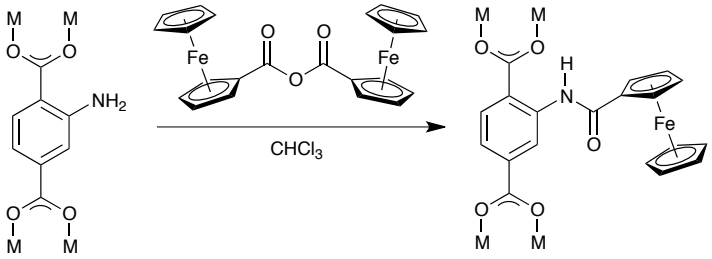

Scheme 1. Post-synthetic modification of an amine-functionalised MOF to give a ferrocenyl amide functionalised MOF.

Compound **1** reacts with FCA to form the ferrocenyl-functionalised derivative **1-Fc**. When **1** was treated with FCA at room temperature in $CHCl_3$ for 3 days, functionalisation occurred with only 3-4% conversion of amines to amide groups. Increasing the temperature to 100 °C led to a slight increase in conversion, but only to 5%. These results suggested that the pores in **1** were not very accessible to the FCA molecules, and it is notable that the degree of amine to amide conversion in other systems falls strongly with an increase in reagent chain length.[31]

Compound **2** has larger pores than **1**, and previous work has shown that this leads to higher degrees of post-synthetic modification.[24] Similarly, the longer linkers in **3** would be expected to facilitate greater access of the reagent into the pores.[28] However, when either **2** or **3** were treated with FCA at room temperature in $CHCl_3$, no presence of the amide was observed after 3 days. In contrast, when the samples were heated at 100 °C, the anticipated greater conversions were observed, with between 17 and 31 % conversion to the amide achieved for modification of **2** into **2-Fc** and 100 % conversion achieved for the modification of **3** into **3-Fc**. In both cases,

the ferrocenyl regions of the ^{1}H NMR spectra of the DCl-digested MOFs show low intensity peaks consistent with the presence of ferrocenecarboxylic acid in addition to the peaks assigned to the modified benzenedicarboxylic acid D_2bdc-NHC(O)C_5H_4FeCp. These may arise from hydrolysis of the amide during digestion, or alternatively some ferrocenylcarboxylic acid may be present as a by-product of the post-synthetic modification process. Similar observations have been reported with other amine to amide conversions.[24, 31] Given the results from the voltammetric studies (*vide infra*) the possible presence of ferrocenecarboxylic acid in the pores is not believed to be significant in the resulting solid state redox properties.

The aluminium MOF **4** reacted with FCA to give the ferrocenyl amide derivative **4-Fc**, but in this case it is more difficult to assess the degree of conversion. **4-Fc** does not dissolve sufficiently in DCl/d_6-dmso for ^{1}H NMR analysis, and although it does dissolve in NaOH/D_2O, the more forcing conditions lead to hydrolysis of the amide. While it is not possible to know the degree of modification, there is strong spectroscopic evidence that significant conversion has occurred. In the infrared spectra, the observation of new bands at 3673 and 1698 cm^{-1} are consistent with the formation of an amide group.[32] In addition, the negative mode ESI mass spectrum of the HCl(aq) partially digested sample of **4-Fc** shows a peak at *m/z* 392.0211 which is indicative of the ferrocenyl amide-modified linker (calc. 392.0227 for [Hbdc-NHC(O)C_5H_4FeCp]$^-$).

Of the ferrocenyl-modified MOFs, **2-Fc** and **4-Fc** were selected for electrochemical study due to their known structures, significant conversion and their moisture stability. Figure 1 shows suggested pore structures for these modified MOFs. The

post-synthetic modification of **4** requires rotation of the benzene ring out of the plane defined by the carboxylate groups in order to accommodate the amidoferrocenyl group.

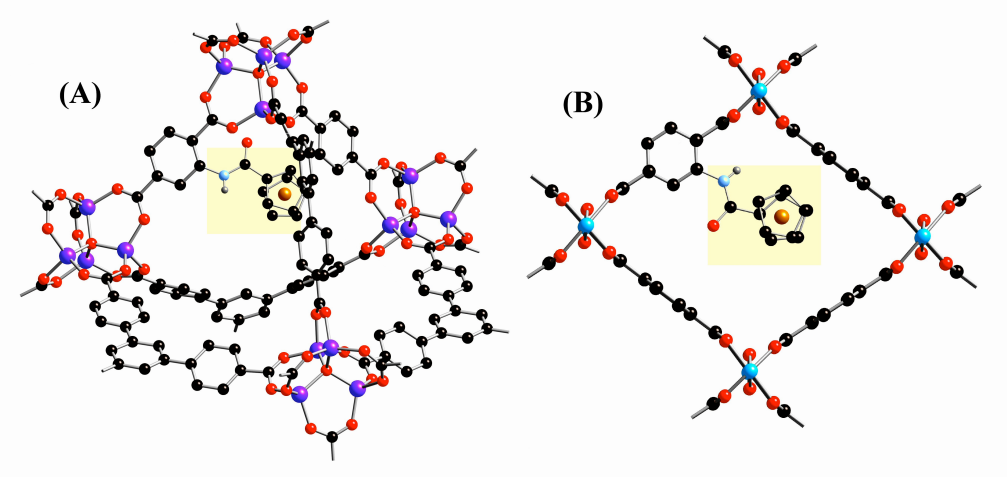

Figure 1. (A) Suggested pore structures of the ferrocenyl-modified MOFs (A) $[Zn_4O(bdc\text{-}NH_2)_{1-x}\{bdc\text{-}NHC(O)Fc\}_x(btb)_{4/3}]$ **2-Fc** (btb = 1,3,5-benzenetribenzoate, Fc = $C_5H_4Fe(C_5H_5)$), and (B) $[Al(OH)(bdc\text{-}NH_2)_{1-x}\{bdc\text{-}NHC(O)Fc\}_x]$ **4-Fc**.

3.2. Voltammetric Study of 2-Fc in Aqueous Electrolyte

The micropowder of **2-Fc** was attached to a basal plane pyrolytic graphite electrode and studied in aqueous electrolyte solution. In 0.1 M phosphate buffer pH 1 (see Figure 2A) a set of at least two distinct processes is observed. Process 1 appears at 0.4 V vs. SCE as a reversible oxidation response and when investigated over a limited potential range from 0.0 to 0.6 V *vs.* SCE this process slowly decays within approximately 10 potential cycles. The process is likely to be associated with "near-surface" immobilised ferrocene. When studied over a range of pH values (see Figure 2C-E) weak pH dependence with approximately 30 mV shift per pH unit is observed. It is likely that this pH dependence is caused by the MOF framework rather than by the ferrocene redox process directly (*vide infra*).

A second oxidation process (see process 2 in Figure 2A) occurs at ca. 0.7 V *vs.* SCE with a higher peak current. This oxidation response appears chemically irreversible and the signal is decaying within a few potential cycles. The charge under this oxidation peak response is approximately one order of magnitude higher when compared to that for process 1 and therefore a bulk process with conversion of the **2**-Fc micropowder is proposed. The effect of pH on this redox process is similar compared to that observed for process 1 (see Figure 2F) and therefore a similar overall effect of the MOF framework appears likely.

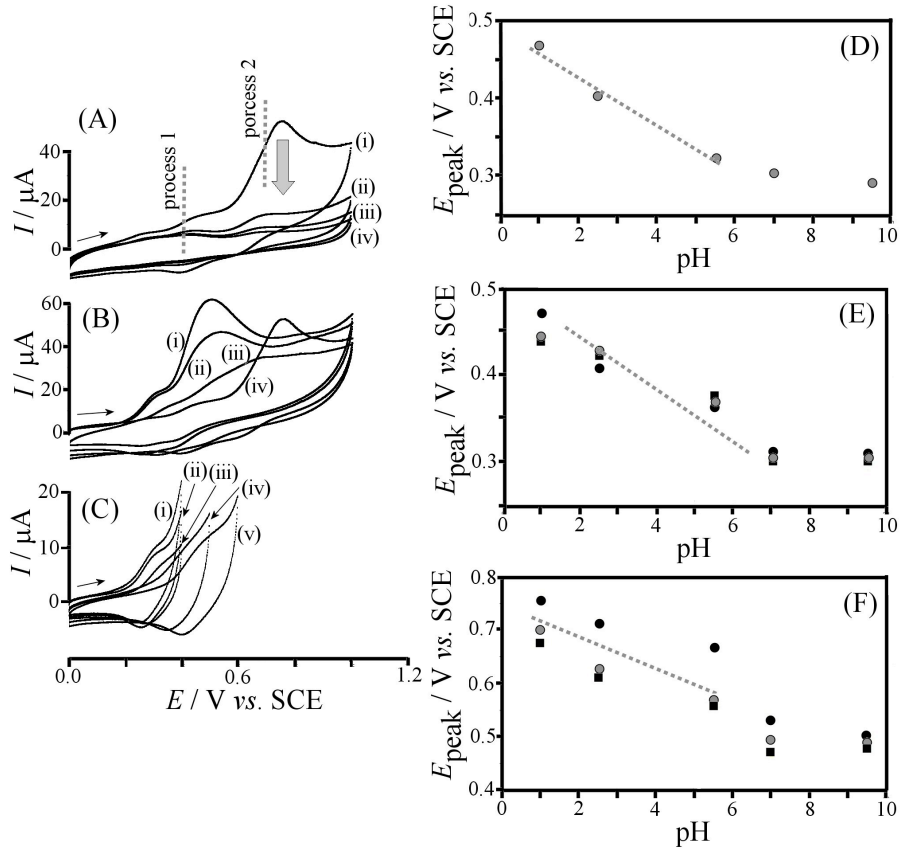

Figure 2. (A) Cyclic voltammograms (scan rate 20 mVs^{-1}, the first four scans shown) for the oxidation of **2-Fc** powder immobilised at a bppg electrode and immersed in aqueous 0.1 M phosphate buffer pH 1. (B) Cyclic voltammograms obtained at pH (i) 9.5, (ii) 7.0, (iii) 5.5, and (iv) 1.0. (C) Cyclic voltammograms obtained at pH (i) 9.0, (ii) 7.0, (iii) 5.0, (iv) 3.0, and (v) 1.0. (D) Plot of the process 1 peak potential versus pH. (E) Plot of the process 1 peak potential (scan 1-3) versus pH. (F) Plot of the peak potential for process 2 versus pH. Dashed lines indicate 30 mV pH^{-1}.

The magnitude of the pH effect, *ca.* 30 mV per pH unit, implies that less than one proton/hydroxide is involved per electron transferred and this may be interpreted in terms of a spatial effect. For the outer-most ferrocenyl groups no pH effect is anticipated due to other ions from solution being accessible. But for ferrocenyl-groups deeper within the MOF framework pH effects due to the high mobility of protons may arise. The observed effect is likely to be caused by a transition in mechanism going from the MOF particle surface into the interior. The resulting formation of hydroxide within pores is discussed below.

Due to the rapid decay of the voltammetric signal for **2-Fc** in aqueous buffer media more detailed investigation of the effect of scan rate is not possible. However, the effect of the supporting electrolyte was investigated for 0.1 M $NaClO_4$, 0.1 M KCl, and 0.1 M tetramethylammonium chloride. Data for these experiments are in close agreement with the voltammetric data obtained for phosphate buffer and therefore effects caused by these electrolyte anions and cations seem insignificant. The ferrocene-centered redox process appears to involve predominantly protons and/or hydroxide and the MOF framework in the charge compensation process (*vide infra*). The expulsion of a proton (the most mobile species) from the MOF host upon ferrocene oxidation appears likely.

3.3. Voltammetric Study of 2-Fc in Organic Electrolyte

Next, voltammetric measurements are carried out in a water-free and "mild" dichloroethane 0.1 M NBu_4PF_6 electrolyte solution. By avoiding exposure to nucleophilic reagents and moisture the ferrocene redox probe can be protected against

oxidative degradation and the MOF framework stabilised. A single voltammetric response for the oxidation of **2-Fc** is observed at 0.68 V *vs.* SCE (see Figure 3A) consistent with process 2 in aqueous media. However, this oxidation and back-reduction process is observed without significant decay of the voltammetric response and therefore investigated here in more detail.

The position of the oxidation and reduction peak responses appears to be independent of the scan rate (see Figure 3B) indicative of fast electron transfer limited by transport or finite diffusion. The investigation of the peak current as a function of scan rate (see Figure 3C) results in a dependence of approximately $I_{peak} \sim (\text{scan rate})^{0.78}$ which is indicative of almost completely finite diffusion. There could be many smaller particles with complete oxidation of the surface and a few larger aggregates or particles which are not fully surface-oxidised within the experimental time scale. The peak-to-peak separation of *ca.* 100 mV could suggest some structural rearrangement during oxidation and back-reduction or the presence of distinct sites.

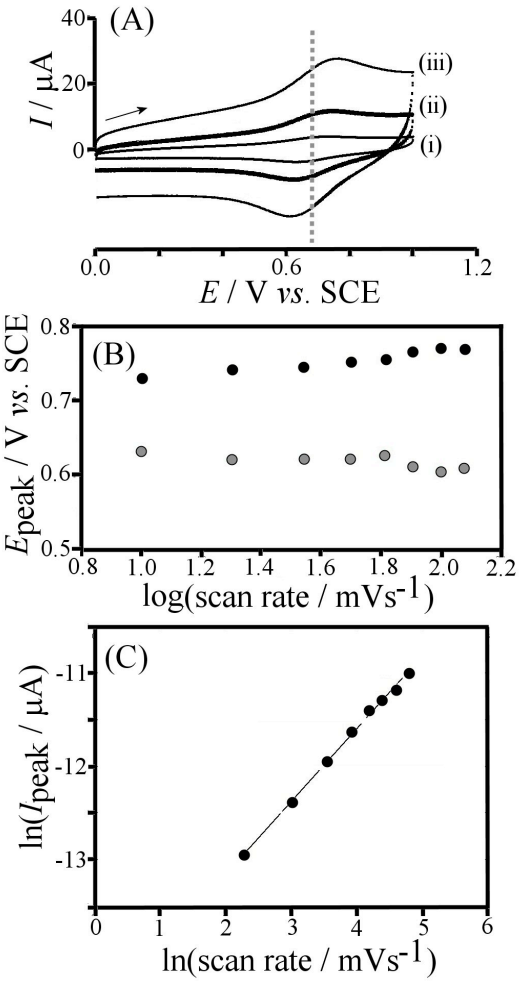

Figure 3. (A) Cyclic voltammograms (scan rate (i) 10, (ii) 35, and (iii) 100 mV s^{-1}) for the oxidation of **2-Fc** powder immobilized at bppg and immersed into dichloroethane with 0.1 M NBu_4PF_6. (B) Plot of the oxidation and reduction peak potentials versus logarithm of scan rate. (C) Plot of the logarithm of anodic peak current versus the logarithm of scan rate with a line of slope 0.78.

The magnitude of the peak currents for oxidation and for reduction (and the charge under the peaks) in this case are considerably lower compared to those observed in aqueous media (see Figure 2A) and therefore a partial conversion appears to occur. Most likely is a surface-confined redox process where particle surface are oxidized but the bulk interior remains unaffected. The mobility of charges at the **2-Fc** | organic electrolyte interface appears high and hopping conduction through a surface layer appears most likely as the mechanism.

3.4. Voltammetric Study of 4-Fc in Aqueous Electrolyte

When immobilised onto bppg electrode surfaces and immersed into aqueous buffer solution, very similar voltammetric responses were observed for **4-Fc** as for **2-Fc**. Data in Figure 4A demonstrates that there are processes similar to process 1 and process 2 with rapid decay of the signals in consecutive potential cycles. The voltammetric responses in this case are less informative due to rapid decay after oxidation. Process 1 appears to be again weakly pH dependent (see Figure 3B).

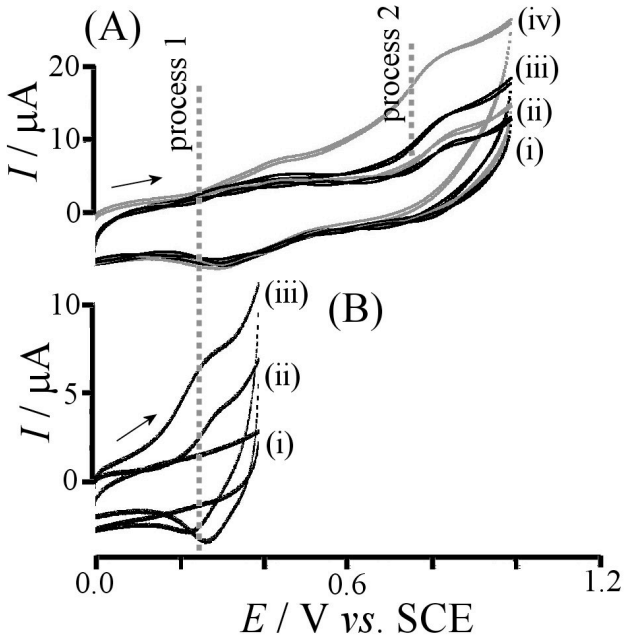

Figure 4. (A) Cyclic voltammograms (scan rate 20 mV s^{-1}) for the oxidation of **4-Fc** powder immobilised at a bppg electrode and immersed into aqueous phosphate buffer pH 9. (B) Cyclic voltammograms (scan rate 15 mVs^{-1}, pH (i) 5, (ii) 7, (iii) 9) for the oxidation of **4-Fc** in phosphate buffer.

3.5. Voltammetric Study of 4-Fc in Organic Electrolyte

Next, the **4-Fc** micropowder was investigated in dichloroethane 0.1 M NBu_4PF_6 as a milder environment. A stable voltammetric response was observed with E_{mid} 0.68 V *vs.* SCE. This process is consistent with that observed for **2-Fc**.

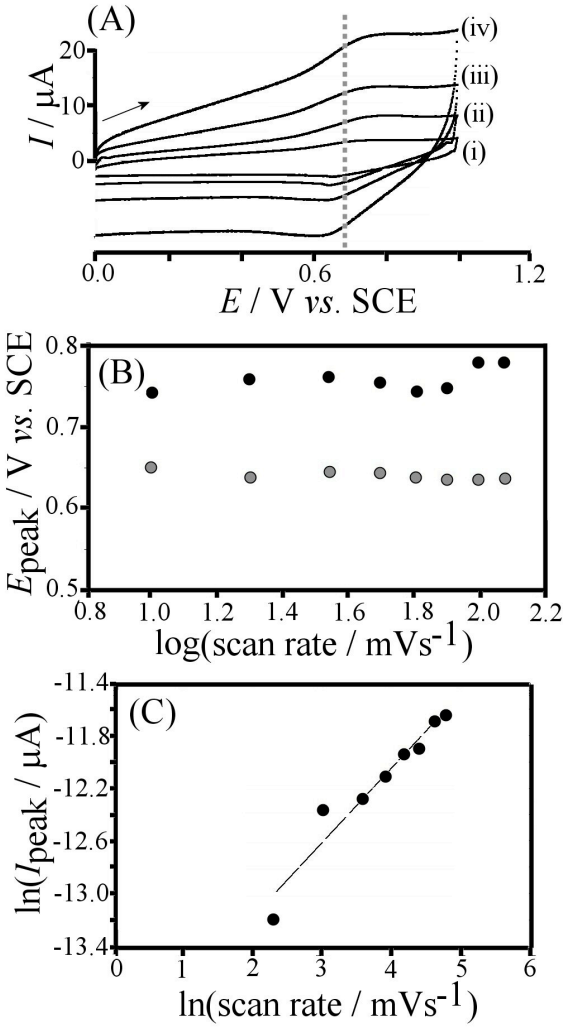

Figure 5. (A) Cyclic voltammograms (scan rate (i) 10, (ii) 20, (iii) 50, and (iv) 100 mV s^{-1}) for the oxidation of **4-Fc** powder immobilized at bppg and immersed into dichloroethane with 0.1 M NBu_4PF_6. (B) Plot of the oxidation and reduction peak potentials versus logarithm of scan rate. (C) Plot of the logarithm of anodic peak current versus the logarithm of scan rate with a line of slope 0.56.

The peak to peak separation appears essentially independent of the scan rate at 120 mV (see Figure 5B). The plot of the logarithm of peak current versus logarithm of scan rate suggests that I_{peak} ~ (scan rate)$^{0.56}$ consistent with more semi-infinite diffusion of charges across the micro-particle surfaces.

Figure 6 shows diagrammatic interpretation of the voltammetric data for **2-Fc** and for **4-Fc** redox reactivity in aqueous and in organic electrolyte media. It is proposed that in aqueous media the ferrocene oxidation within pores is associated with expulsion of protons from the framework structure. The resulting hydroxide ions could considerably weaken the framework and cause (electro-chemically driven) disintegration.

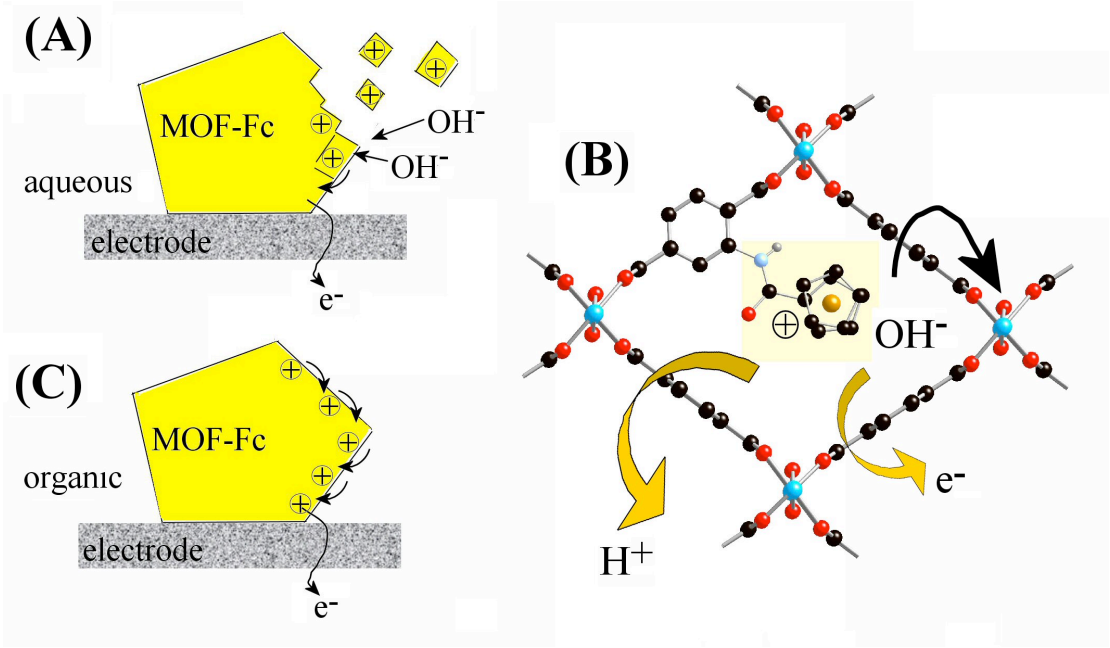

Figure 6. (A) Schematic description of the ferrocenyl MOF reactivity in aqueous media. (B) Drawing of the pore redox process involving (i) removal of one electron, (ii) fast expulsion of one proton, and (iii) attack of the hydroxide on the framework. (C) Schematic description of the ferrocenyl MOF reactivity in organic media.

It is interesting to note that the anticipated ion insertion chemistry for MOFs (as known for example for Prussian blue materials[33, 34]) is indeed related to these disintegration processes. For materials where electrochemical framework rupture is accompanied by re-precipitation or "healing", process 2 would result in a net ion insertion process. However, for the cases investigated here, the zinc and aluminium MOF frameworks do not re-assemble due to solubility of the ferrocenyl-modified benzenedicarboxylate ligands in the aqueous environment. MOF materials with "self-healing" frameworks will be of interest in future applications for example in energy storage.

4. Summary

It has been demonstrated that amine-functionalised MOFs can be post-synthetically modified to form MOFs in which ferrocenyl groups are tethered to the framework backbone. These MOFs have been shown to act as novel redox active materials. In organic media, well-defined and stable redox processes are observed associated with the oxidation and back-reduction of the pore surface ferrocenes. Rapid hopping of charges across the MOF surface has been proposed to account for the magnitude and scan rate dependence of the signals. However, in aqueous media voltammetric responses for the ferrocene oxidation exhibit rapid decay due to dissolution of the functionalised MOF framework. The pH effect on the voltammetric responses has been interpreted in terms of a "framework effect" where hydroxide attack on the framework metal centre can "compensate" the positive charge from interstitial ferrocenium. Insight into the aqueous and organic redox reactivity in these two cases will lead to further developments of functional redox-active MOFs.

Acknowledgement

JEH thanks the University of Bath and EPSRC for a studentship. AH-G thanks the Ministerio de Ciencia e Innovacion in Spain for a grant to support his stay in Bath.

References

1. J. L. C. Rowsell and O. M. Yaghi, *Micropor. Mesopor. Mat.*, 2004, **73**, 3.
2. G. Férey, *Chem. Soc. Rev.*, 2008, **37**, 191.
3. S. Horike, S. Shimomura and S. Kitagawa, *Nature Chem.*, 2009, **1**, 695.
4. A. U. Czaja, N. Trukhan and U. Müller, *Chem. Soc. Rev.*, 2009, **38**, 1284.
5. K. K. Tanabe and S. M. Cohen, *Chem. Soc. Rev.*, 2011, **40**, 498.
6. A. Doménech-Carbó, *Electrochemistry of Porous Materials*, CRC Press, London, 2010, 95.
7. A. Doménech, H. García, M. T. Doménech-Carbó and F. Llabrés-i-Xamena, *J. Phys. Chem. C*, 2007, **111**, 13701.
8. R. C. Millward, C. E. Madden, I. Sutherland, R. J. Mortimer, S. Fletcher and F. Marken, *Chem. Commun.*, 2001, 1994.
9. H. Lin, X. Wang, H. Hu, B. Chen and G. Liu, *Solid State Sci.*, 2009, **11**, 643.
10. L. M. Rodriguez-Albelo, A. R. Ruiz-Salvador, A. Sampieri, D. W. Lewis, A. Gómez, B. Nohra, P. Mialane, J. Marrot, F. Sécheresse, C. Mellot-Draznieks, R. N. Biboum, B. Keita, L. Nadjo and A. Dolbecq, *J. Am. Chem. Soc.*, 2009, **131**, 16078.
11. K. L. Mulfort and J. T. Hupp, *J. Am. Chem. Soc.*, 2007, **129**, 9604.

12. T. L. A. Nguyen, T. Devic, P. Mialane, E. Rivière, A. Sonnauer, N. Stock, R. Demir-Cakan, M. Morcrette, C. Livage, J. Marrot, J.-M. Tarascon and G. Férey, *Inorg. Chem.*, 2010, **49**, 10710.

13. Y. R. Qin, Q. Y. Zhu, L. B. Huo, Z. Shi, G. Q. Bian and J. Dai, *Inorg. Chem.*, 2010, **49**, 7372.

14. K. F. Babu, M. A. Kulandainathan, I. Katsounaros, L. Rassaei, A. D. Burrows, P. R. Raithby and F. Marken, *Electrochem. Commun.*, 2010, **12**, 632.

15. L. Yang, S. Kinoshita, T. Yamada, S. Kanda, H. Kitagawa, M. Tokunaga, T. Ishimoto, T. Ogura, R. Nagumo, A. Miyamoto and M. Koyama, *Angew. Chem. Int. Ed.*, 2010, **49**, 5348

16. R. Horikoshi and T. Mochida, *Eur. J. Inorg. Chem.*, 2010, 5355.

17. S. Hermes, F. Schröder, S. Amirjalayer, R. Schmid and R. Fischer, *J. Mater. Chem.*, 2006, **16**, 2464.

18. M. Müller, O. I. Lebedev and R. A. Fischer, *J. Mater. Chem.*, 2008, **18**, 5274.

19. M. Meilikhov, K. Yusenko and R. A. Fischer, *Dalton Trans.*, 2009, 600.

20. M. Meilikhov, K. Yusenko and R. A. Fischer, *Dalton Trans.*, 2010, **39**, 10990.

21. Y. K. Park, S. B. Choi, H. Kim, K. Kim, B.-H. Won, K. Choi, J.-S. Choi, W.-S. Ahn, N. Won, S. Kim, D. H. Jung, S.-H. Choi, G.-H. Kim, S.-S. Cha, Y. H. Jhon, J. K. Yang and J. Kim, *Angew. Chem. Int. Ed.*, 2007, **46**, 8230.

22. M. Meilikhov, K. Yusenko and R. A. Fischer, *J. Am. Chem. Soc.*, 2009, **131**, 9644.

23. M. Eddaoudi, J. Kim, N. Rosi, D. Vodak, J. Wachter, M. O'Keeffe and O. M. Yaghi, *Science*, 2002, **295**, 469.

24. Z. Wang, K. K. Tanabe and S. M. Cohen, *Inorg. Chem.*, 2009, **48**, 296.

25. T. Ahnfeldt, D. Gunzelmann, T. Loiseau, D. Hirsemann, J. Senker, G. Férey and N. Stock, *Inorg. Chem.*, 2009, **48**, 3057.

26. R. K. Deshpande, J. L. Minnaar and S. G. Telfer, *Angew. Chem. Int. Ed.*, 2010, **49**, 4598.

27. T. Grygar, F. Marken, U. Schröder and F. Scholz, *Collect. Czech. Chem. Commun.*, 2002, **67**, 163.

28. A. D. Burrows, C. G. Frost, M. F. Mahon and C. Richardson, *Angew. Chem. Int. Ed.*, 2008, **47**, 8482.

29. A. D. Burrows, C. G. Frost, M. F. Mahon and C. Richardson, *Chem. Commun.*, 2009, 4218.

30. Z. Wang and S. M. Cohen, *J. Am. Chem. Soc.*, 2007, **129**, 12368.

31. K. K. Tanabe, Z. Wang and S. M. Cohen, *J. Am. Chem. Soc.*, 2008, **130**, 8508.

32. M. Oberhoff, L. Duda, J. Karl, R. Mohr, G. Erker, R. Fröhlich and M. Grehl, *Organometallics*, 1996, **15**, 4005.

33. K. Itaya, I. Uchida and V. D. Neff, *Acc. Chem. Res.*, 1986, **19**, 162.

34. R. J. Mortimer, *Chem. Soc. Rev.*, 1997, **26**, 147.